

## CHAPTER 146

### MEASUREMENT OF REFLECTION COEFFICIENT

#### OF SEAWALL IN OMURA BAY

by

Kosuke Kondo<sup>\*</sup>, Masayuki Akama<sup>\*\*</sup> and Masahiko Isobe<sup>\*\*\*</sup>

#### ABSTRACT

Field investigations were performed in order to establish the reflecting characteristics of a steel sheet-piling type seawall and two vertical wave-dissipating type seawalls through directional wave measurements of wave reflection systems. A pre-designed line array of several capacitance-type wave gauges was used to measure the wave field just in front of the seawall, and the MMLM (Modified Maximum Likelihood Method) was applied for the calculation of the directional wave spectrum and the reflection coefficient. The estimated directional spectra demonstrated that the MMLM has high resolution power and can sufficiently separate the incident and the reflected wave energies. As a result, it was found that the reflection coefficient of the vertical steel sheet-piling seawall is about 0.9 and is independent of the incident wave conditions, whereas those of the vertical wave-dissipating type seawalls show considerable change in correlation to the incident wave period or the mean water level.

#### 1. INTRODUCTION

Many types of wave-dissipating vertical seawall structures have recently been constructed in Japan in order to reduce the effect of reflected waves from these structures. In designing and constructing them, it is necessary to estimate the reflective characteristics of these structures.

Laboratory flume tests are often performed using a scale model of a seawall. Actual reflection coefficients are, however, expected to be different from those obtained in laboratory flumes because actual sea waves are directionally spread and so measuring the reflection coefficient of seawalls in the field is of great importance.

---

\* Principal Engineer, Design and Engineering Department, Penta-Ocean Construction Co., Ltd., 2-2-8 Koraku, Bunkyo-ku, Tokyo, 112 Japan.

\*\* Engineer, Design and Engineering Department, Penta-Ocean Construction Co., Ltd., 2-2-8 Koraku, Bunkyo-ku, Tokyo, 112 Japan.

\*\*\* Associate Professor, Department of Civil Engineering, Yokohama National University, 156 Tokiwadai, Hodogaya-ku, Yokohama, 240 Japan.

The following methods have been examined in the field to know the reflection coefficient of prototype structures (Goda, 1985):

- 1) simultaneous measurement of the wave height  $H_s$  in front of a structure (at a distance more than one wave length from the structure) and the incident wave height  $H_i$  at a location free from the effect of reflected waves;
- 2) measurement of the directional wave spectrum sufficiently far from the reflective structure where the effect of phase-locking of incident and reflected waves becomes negligible; and
- 3) application of the method for resolving the incident and reflected wave spectra in a wave flume by using the autocorrelation function (Kajima, 1969) or the fast Fourier transform technique (Goda and Suzuki, 1976).

These methods have, however, the following problems. By the method 1, the reflection coefficient is affected too much by a slight change of wave height ratio  $H_s/H_i$ . For example, 10% error of  $H_s/H_i$  changes the reflection coefficient between 0.1 and 0.7 when the actual reflection coefficient is 0.5. In using the method 2, the dispersion of waves reflected from a finite length of reflective structure has to be considered. The method 3 is only applicable when waves incident to a structure with narrow directional spreading and the mean direction is almost perpendicular to the structure.

Recently, Isobe and Kondo (1984) presented a theory named MMLM (Modified Maximum Likelihood Method) to measure the directional wave spectrum in a wave reflection system and to determine the reflection coefficient of a structure in a directional sea. The object of this study is to confirm the applicability of the MMLM to the field data and to establish the reflecting characteristics of three different types of seawalls through directional wave measurements of wave reflection systems in the field.

## 2. FIELD INVESTIGATIONS

### 2.1 Site Description

The field investigations were performed on the eastern shore of Omura Bay, Nagasaki Prefecture, Kyushu, Japan in March, 1982 and in January, 1984. A location map of the investigation site is shown in figure 1. Omura Bay is almost entirely separated from the open sea by the surrounding topography. The scale of the bay is about 20 km north to south and about 10 km east to west. The wave climate is very mild throughout most of the year. The exception is winter when the north-west monsoon sometimes blows and wind waves develop.

During the first investigation in 1982, data for a vertical steel sheet-piling type seawall was collected. After this investigation, two vertical wave-dissipating type seawalls (Type A and Type B) were constructed. In 1984, about half a year after the seawalls were constructed, the second investigation was carried out in order to collect the data for the newly constructed seawalls.

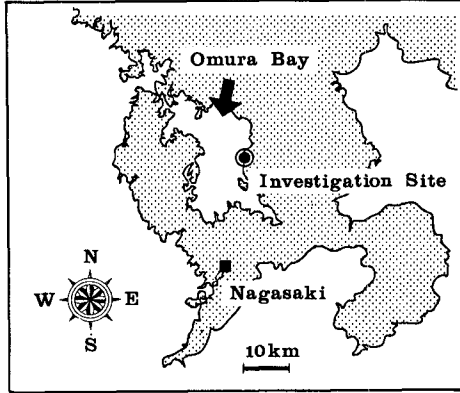


Fig. 1 Location map of the investigation site.

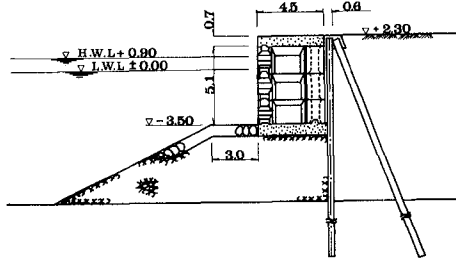
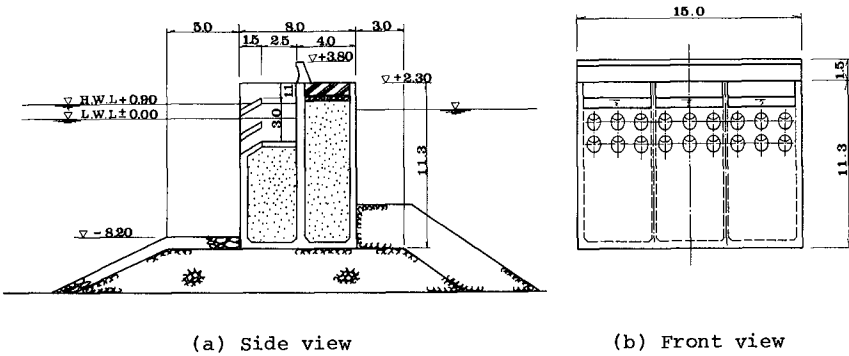


Fig. 2 Schematic profile of the Type A wave-dissipating seawall.



(a) Side view

(b) Front view

Fig. 3 Schematic profile of the Type B wave-dissipating seawall.

Schematic profiles of these vertical wave-dissipating type seawalls are given in figures 2 and 3. Type A is a block type. Three concrete blocks with wave chambers are piled up just in front of the steel sheet-piling wall. Type B is a caisson type. As seen in the front view, this type has many sloping holes in its front wall.

## 2.2 Field Investigation Program

- The field investigation program consisted of these three items:
- 1) measurements of incident and reflected waves in front of the seawall by a line array using three to five capacitance-type wave gauges arranged perpendicular to the wall;
  - 2) measurements of incident waves in the location free from the effect of reflected waves by a line array using two to four capacitance-type wave gauges arranged nearly perpendicular to the wind direction; and
  - 3) measurements of wave height distribution within 1 km of the seawalls using a floating buoy with a twice electronically integrated accelerometer or ultrasonic wave gauges.

In the first investigation, three capacitance-type wave gauges were installed with the distances of 10.0 m, 11.2 m and 13.6 m away from the steel sheet-piling wall respectively, and two capacitance-type wave gauges with an interval of 1.2 m each other were placed about 2 km north of the seawall. The location and arrangement of the wave gauges in the second investigation is explained in figure 4. Five capacitance-type wave gauges were installed just in front of each vertical wave-dissipating type seawall. The incident wave measuring point was located about 2 km north of the seawalls as was in the first investigation, and four capacitance-type wave gauges were arranged with intervals of 2.4 m, 3.6 m and 1.2 m.

A truck-crane was used at the seawalls to support the beam from which wave gauges hung. Several red and white poles were placed at regular intervals between the wave gauges to determine the details of wave height distribution within one wave length of the seawall. This was filmed with a 16 mm motion camera. At the incident wave measuring point, a small self-elevating platform was used. The wind speed and direction were measured at the level of 10 m over the ground surface at the north corner of the reclaimed area.

The arrangement of wave gauges just in front of the seawalls in the second investigation was decided by numerical simulation so as to achieve a high resolution power of the directional wave spectrum and high accuracy in estimating the reflection coefficient. Details about the procedure for this numerical simulation will be explained later.

Every analogue record of approximately 5 minutes length was converted to digital record with a sampling interval of 0.1 second. All data were analyzed statistically, including the calculation of significant wave height and period by the zero-up-crossing method. The frequency spectra were computed using the fast Fourier transform technique on records of 2048 samplings with an interval of 0.1 second after the correction of mean water level. The effective number of degree of freedom was about 23.

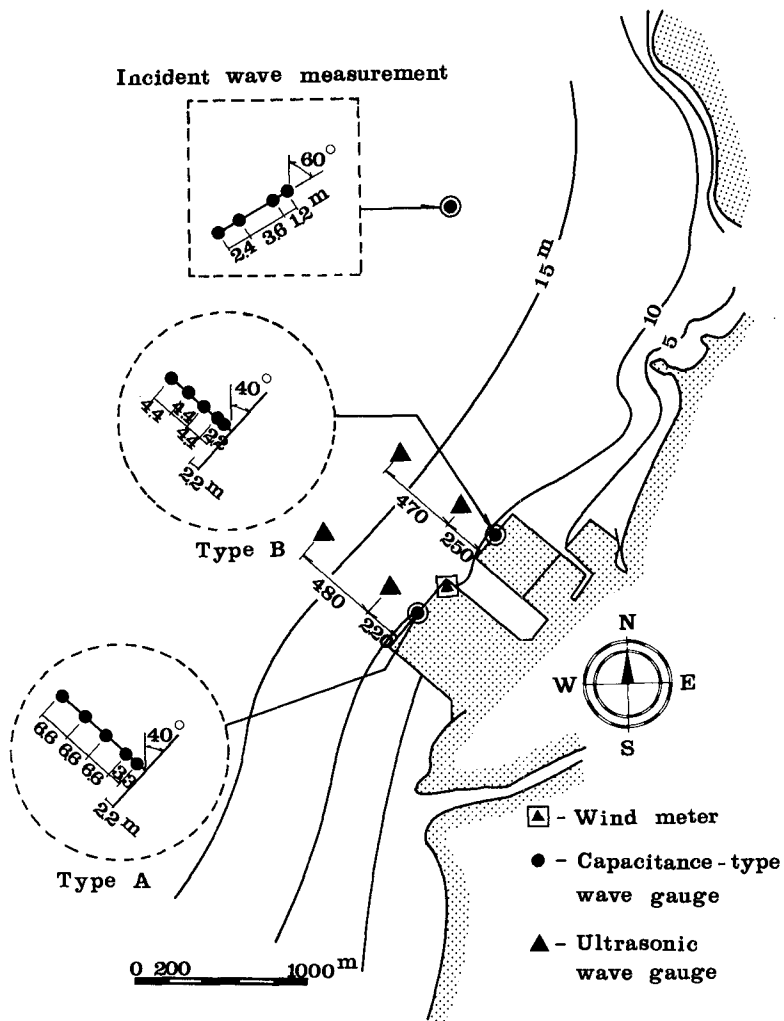


Fig.4 Location and arrangement of the wave gauges in the 2nd investigation.

### 2.3 Wind and Wave Conditions

The wind and wave conditions during the observation periods are shown in figure 5. From the upper side, wind speed, wind direction, wave height, wave period, wave direction and tidal level are presented. Significant wave height reached 0.5 m to 0.8 m in each observation. Significant wave period was 2.5 seconds to 3 seconds. Most of the observed frequency spectra had the shape that indicated greater part of the energy concentrated around the peak frequency. Wave direction was almost equal to the wind direction, that was north-west, and was nearly perpendicular to the seawalls. The wind conditions in the first investigation changed markedly, whereas in the second investigation rather steady wind conditions prevailed.

Figure 6 compares the height of incident waves and that of waves in front of the seawalls. The incident wave height is indicated by the broken line, and that of waves in front of the seawalls is shown by the black or white circle. The wave height near the seawall is an averaged value of those measured by two or three wave gauges located more than one wave length away from the reflecting surface. In the first investigation, the wave height near the seawall was unexpectedly found to be lower than the incident wave height. This may have been due to the unsteadiness of the wind conditions during the first investigation. Such phenomena were very rare in the second investigation. Comparing the two wave heights in front of the Type A and Type B vertical wave-dissipating seawalls, that of Type A is generally greater, which implies that the reflection coefficient of Type B is smaller than that of Type A.

## 3. DIRECTIONAL WAVE SPECTRUM

### 3.1 Basic Formura for Estimating the Directional Spectrum

In the analysis of the directional spectrum with no reflected waves, all the component waves are assumed to be independent, with random and uniformly distributed phase angles. In analyzing the directional wave spectrum in the wave reflection system, however, the fixed phase relation of each pair of incident and reflected wave components should be considered. Therefore, the Modified Maximum Likelihood Method or MMLM was applied for the calculation of the directional wave spectrum and the reflection coefficient. This method is based on the relationship between the directional spectrum and the cross-power spectrum, with extra terms so called phase interaction terms. A directional wave spectrum and a reflection coefficient can be estimated by these two equations.

$$\frac{\alpha}{\hat{S}(\mathbf{k}, \sigma)} = \frac{\sum_m \sum_n \Phi_{m'n}^{-1} \exp \{i\mathbf{k}(\mathbf{x}_n - \mathbf{x}_m)\}}{\frac{[\sum_m \sum_n \Phi_{m'n}^{-1} [\exp \{i\mathbf{k}(\mathbf{x}_n - \mathbf{x}_{nr})\} + \exp \{i\mathbf{k}(\mathbf{x}_{nr} - \mathbf{x}_m)\}]]^2}{4 \sum_m \sum_n \Phi_{m'n}^{-1} \exp \{i\mathbf{k}(\mathbf{x}_{nr} - \mathbf{x}_{nr})\}}}$$
(1)

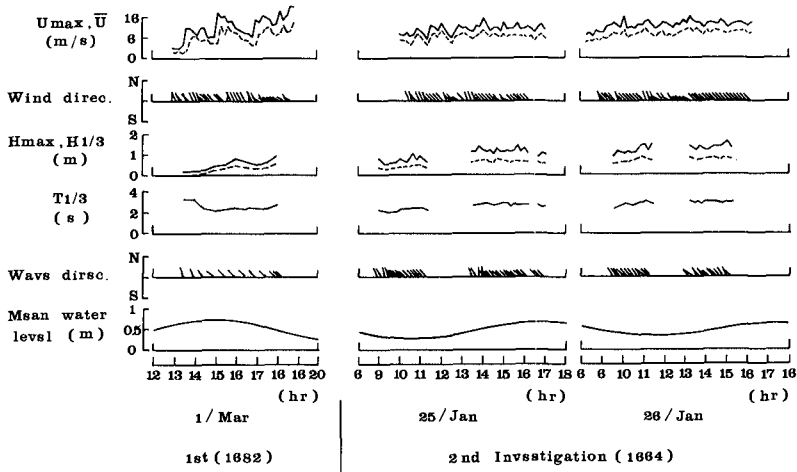


Fig. 5 Wind and wave conditions during the observation period.

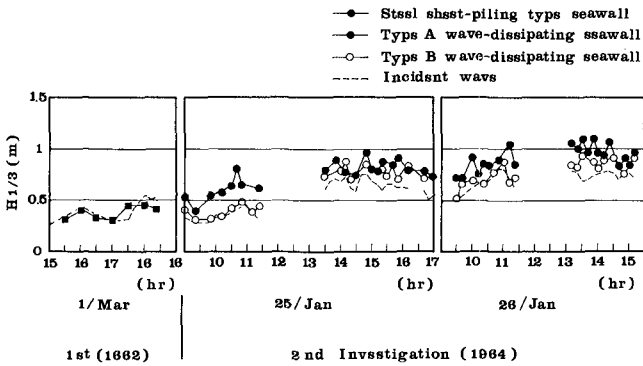


Fig. 6 Comparison between the height of incident waves and that of waves in front of the seawalls.

$$r = - \frac{\sum_m \sum_n \Phi_{mn}^{-1} [\exp \{ik(x_n - x_{mr})\} + \exp \{ik(x_{nr} - x_m)\}]}{2 \sum_m \sum_n \Phi_{mn}^{-1} \exp \{ik(x_{nr} - x_{mr})\}} \quad (2)$$

Where  $\hat{S}(k, \sigma)$  means the estimated wavenumber-frequency spectrum.  $r$  denotes the reflection coefficients.  $\Phi_{mn}(\sigma)$  is the cross-power spectrum of the water surface variations at point  $x_m$  and point  $x_n$ . And  $\alpha$  is a proportionality constant to adjust the power of the spectrum. Without the second term in the right-hand side of equation (1), it completely coincides with that for the standard MLM.

### 3.2 Design of Wave Gauge Array

The resolution power of a directional wave spectrum of the MMLM depends on the number and the arrangement of wave gauges. Therefore, the design of wave gauge array is one of the most important procedure in planning the measurement of the directional wave spectrum and the reflection coefficient. Numerical simulation was performed prior to the second investigation in order to study adequate arrangements of wave gauges. The procedure for the numerical simulation is as follows:

- 1) Specify a form for the directional energy distribution  $S(k, \sigma)$  and the reflection coefficient. Here, the Mitsuyasu-type directional distribution expressed by equation (3) was used. The constant reflection coefficient was assumed for every directional component of waves.

$$S(k, \sigma) = \cos^{2s} \{(\theta - \theta_0)/2\} \quad (3)$$

where  $\theta_0$  is a principal wave direction and  $s$  is a parameter representing the degree of directional energy concentration.

- 2) Calculate  $\Phi_{mn}(\sigma)$  for a given wave gauge array using the relationship between the cross-power spectrum and the directional wave spectrum in an incident and reflected wave field, which is expressed by equation (4).

$$\begin{aligned} \Phi_{mn}(\sigma) = & \int_{\mathbf{k}} S(\mathbf{k}, \sigma) \\ & \times \{ \exp(ikx_m) + r \exp(ikx_{mr}) \} \\ & \times \{ \exp(-ikx_n) + r \exp(-ikx_{nr}) \} d\mathbf{k} \end{aligned} \quad (4)$$

- 3) Estimate the directional energy distribution from equation (1) and compare to the given one.

A line array with four wave gauges which has a pattern described in figure 7 was analyzed by the numerical simulation, using the values of the parameter  $s$  of 5 and 50. In figure 7,  $\Delta x$  is the distance between the first wave gauge and the reflective wall and  $D$  is the basic distance between the first and the second wave gauges. The third is located at  $2D$  away from the second and the last is at  $4D$  from the third.

The results indicated that the arrangement, in which  $\Delta x$  is less than  $0.5L$  and  $D$  is between  $0.2L$  and  $0.3L$ , is effective for wide range of wave length. In the investigation, one more wave gauge was placed at the middle of the third and the last wave gauges.

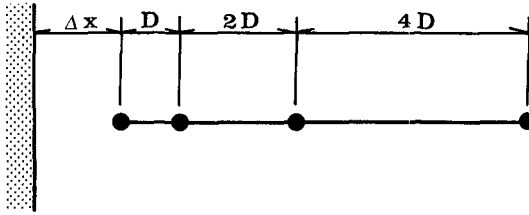


Fig. 7 Definition sketch of wave gauge array

### 3.3 Analysis of Field Data

Figure 8 shows some examples of the directional wave spectrum estimated from field data with MLM. These are derived by integrating the wavenumber-frequency spectrum with respect to the frequency. The energy level is normalized by the total wave energy. The directional wave spectra for the incident waves, for the waves in front of the Type A and for the waves in front of the Type B seawall are compared.  $0^\circ$  and  $180^\circ$  are parallel with the line array of wave gauges. These directions are simultaneously perpendicular to the seawall line in figures 8(b) and 8(c).

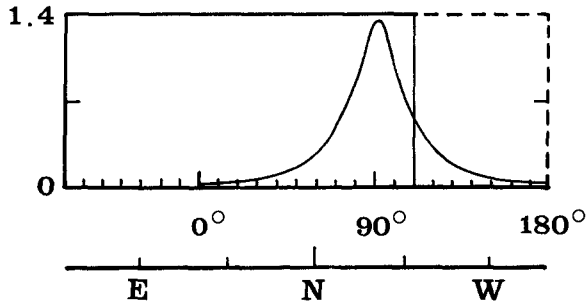
At the incident wave measuring point, the wave direction is nearly perpendicular to the line array and most of the energy concentrates around the peak direction. The estimated directional wave spectrum in front of a seawall has two peaks in the symmetrical positions of  $90^\circ$ , corresponding to the incident and the reflected waves. The directional peaks of the incident and the reflected waves are sufficiently separated.

An example of the normalized directional energy distribution for each frequency is shown in figure 9. The graphs are arranged from bottom to top and from left to right, as the frequency increases. The peak frequency of wave energy is around 0.32 Hz. The separation of the incident waves and the reflected waves is good enough for each frequency.

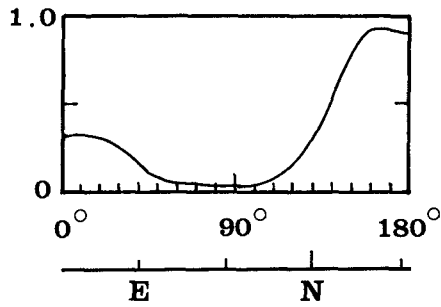
## 4. REFLECTION COEFFICIENT

### 4.1 Definition of Reflection Coefficient

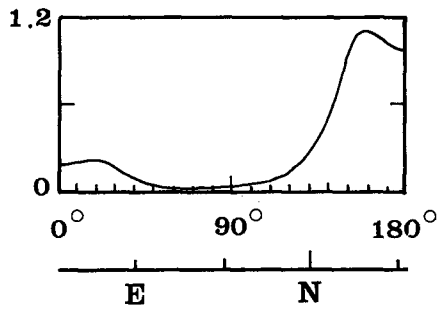
In estimating the reflection coefficient, the following two methods were compared. Equation (2) gives an estimation of the reflection coefficient for each frequency and for each direction. The first method is to adopt this one at the peak frequency and the peak direction. This reflection coefficient is denoted by  $r_p$ . The second



(a) Incident waves



(b) Incident and reflected waves in front of the Type A seawall.



(c) Incident and reflected waves in front of the Type B seawall.

Fig. 8 Examples of estimated directional wave spectrum (1984/1/26, 13:30).

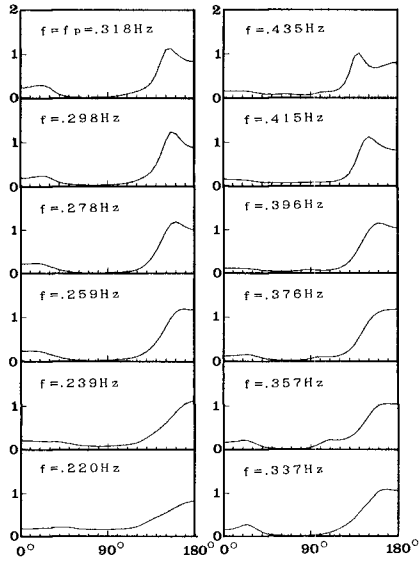


Fig. 9 An example of directional energy distribution for each frequency.

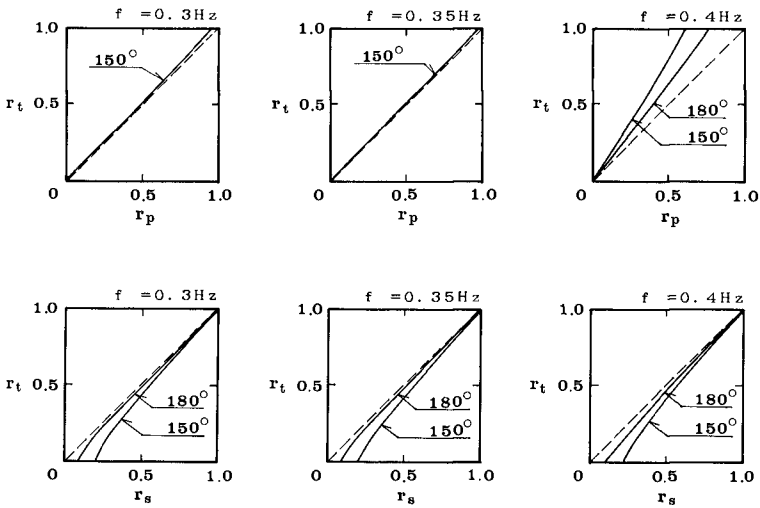


Fig. 10 Comparison between estimated and true reflection coefficients.

method is to adopt the square root of the ratio between the integrated reflected and incident wave energy. This reflection coefficient is denoted by  $\Gamma_s$ . The correspondence between the true reflection coefficient and the estimated one was analyzed by numerical simulation.

The results are presented in figure 10. In each graph the horizontal axis is an estimated reflection coefficient  $\Gamma_p$  or  $\Gamma_s$  and the vertical axis is a true reflection coefficient  $\Gamma_t$ . Three different frequency cases are shown for both  $\Gamma_p$  and  $\Gamma_s$ . The arrangement of wave gauges was assumed as that adopted in front of the Type B seawall. It can be found that  $\Gamma_p$  gives a fairly accurate value for the full range of the reflection coefficient when the peak frequency is between 0.3 and 0.35. Should the peak frequency be 0.4,  $\Gamma_p$  tends to underestimate in the high reflection range. When the true reflection coefficient is larger than 0.5,  $\Gamma_s$  gives a fairly good value for all frequencies.

#### 4.2 Reflecting Characteristics of Seawalls

Table 1 shows the reflection coefficients of the vertical steel sheet-piling seawall estimated for twelve occasions of measurement. The incident wave direction, defined as an angle from the normal direction of the seawall line, varied between  $-20^\circ$  and  $30^\circ$ . The peak frequency of the incident wave was between 0.34 and 0.44. The reflection coefficient is independent of the direction and the peak frequency of the incident wave and shows rather stable values between 0.85 and 1.0 with a mean value of 0.92.

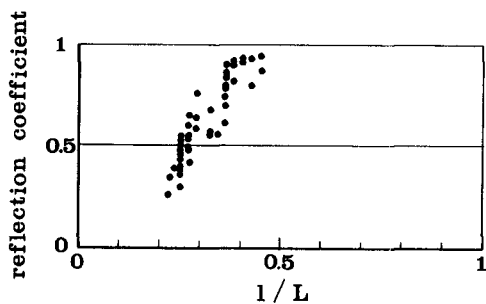
Figure 11 shows the relationship between the relative width of wave chamber to wave length ( $l/L$ ) and the reflection coefficient of the Type A wave-dissipating seawall. The wave length was calculated for the peak frequency of the incident wave. The reflection coefficient shows the minimum value of 0.3 at  $l/L = 0.25$  and the maximum value of 0.9 at  $l/L = 0.5$ . This is the same tendency as was obtained by Tanimoto and Yoshimoto (1982) in the wave flume experiment for a vertical slit caisson (figure 12).

The reflection coefficient of the Type B wave-dissipating seawall was also plotted against  $l/L$ , but there seems to be poor correlation (figure 13). Figure 14 shows the relationship between the mean water level and the reflection coefficient. The reflection coefficient of the Type B doesn't depend on  $l/L$ , but has a good correlation to the mean water level. This is considered to be caused by the relative position of the holes through the front wall of the caisson and the water surface level under the condition of rather low wave height compared to the size of the holes.

The tendencies of the reflection coefficient changes stated above was also confirmed by the results of the wave height distribution measurements carried out simultaneously in the front area of the seawalls.

Table 1 Reflection coefficient of vertical steel sheet-piling type seawall.

time (1/Mar)	reflection coefficient		wave direction (deg)	peak frequency (Hz)
	$r_p$	$r_s$		
15:30	0.96	0.93	25	0.435
16:00	0.84	0.87	20	0.376
16:30	0.86	0.98	20	0.357
16:50	0.89	(1.06)	20	0.357
17:00	0.72	(1.01)	0	0.376
17:10	0.82	0.93	0	0.337
17:20	0.96	0.96	25	0.357
17:30	0.73	0.89	25	0.376
17:40	0.90	0.89	30	0.357
18:00	0.86	0.87	30	0.337
18:10	0.93	0.98	-20	0.347
18:20	0.78	0.90	-20	0.337
mean	0.85	0.92		

Fig. 11 Relationship between relative width of wave chamber( $l$ ) to wave length( $L$ ) and reflection coefficient: Type A seawall.

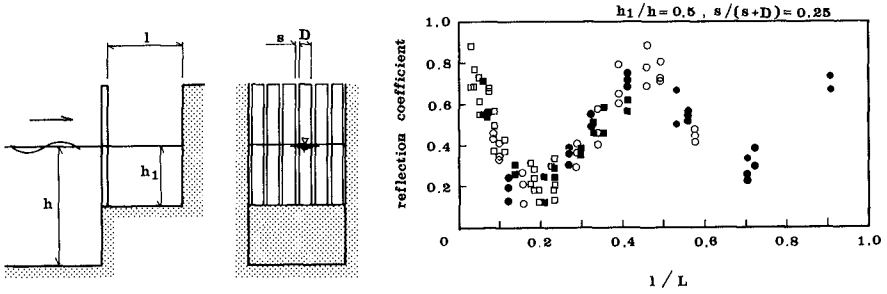


Fig. 12 Relationship between  $l/L$  and reflection coefficient in a flume experiment for a vertical slit caisson :after Tanimoto and Yoshimoto (1982)

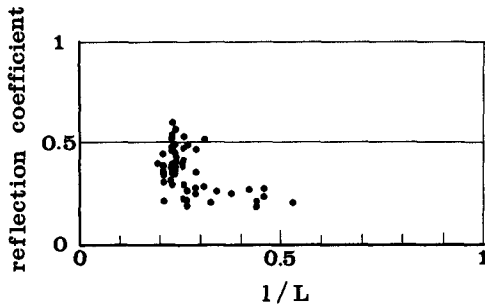


Fig. 13 Relationship between  $1/L$  and reflection coefficient: Type B seawall.

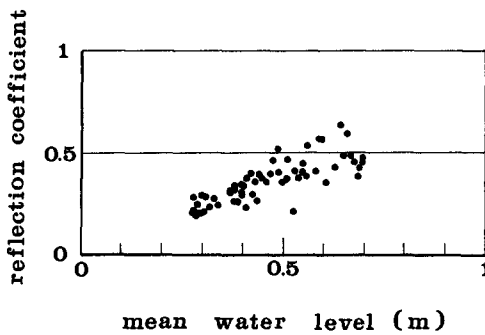


Fig. 14 Relationship between mean water level and reflection coefficient: Type B seawall.

## 5. CONCLUSIONS

The MMLM was applied to the field data in order to estimate the reflection coefficients of three different types of seawalls. The estimated directional wave spectra demonstrated that the MMLM has high resolution power and can sufficiently separate the incident and the reflected wave energies.

As a result, it was found that the reflection coefficient of the vertical steel sheet-piling seawall is about 0.9 and is independent of the direction and the period of the incident wave, whereas those of the vertical wave-dissipating seawalls show considerable change in correlation to the incident wave period or the mean water level.

The design of wave gauge array is one of the most important procedure in planning the measurement of the directional wave spectrum and the reflection coefficient. It was possible in this study to determine the arrangement of wave gauges by numerical simulation so as to achieve a high accuracy in estimating the directional spectrum and the reflection coefficient since the dominant wave period and direction at the study area had been known before the investigation. Much more analysis by numerical simulation and understanding of the applicable limit of a wave gauge array used may be necessary in the measurement in an open sea, where the wave condition changes in a wide range of wave period and direction.

## ACKNOWLEDGEMENTS

The authors express their appreciation to Mr. R. Kajima of the Central Research Institute of Electric Power Industry for his valuable consultation and advice. We would also like to thank Mr. K. Kaneko and Mr. T. Oku of the Kyushu Electric Power Co., Ltd. for their support to this study and for their permission to publish this paper.

## REFERENCES

- 1) Goda, Y. (1985): Random Seas and Design of Maritime Structures, University of Tokyo Press, 323p.
- 2) Goda, Y. and Y. Suzuki (1976): Estimation of Incident and Reflected Waves in Random Wave Experiments, Proc. 15th Int. Conf. Coastal Eng., Hawaii, pp.828-845.
- 3) Isobe, M. and K. Kondo (1984): Method for Estimating Directional Wave Spectrum in Incident and Reflected Wave Field, Proc. 19th Int. Conf. Coastal Eng., Houston, pp.467-483.
- 4) Kajima, R. (1969): Estimation of Incident Wave Spectrum in the Sea Area Influenced by Reflection, Coastal Engineering in Japan, Vol.12, pp.9 - 16.
- 5) Mitsuyasu, H. et al. (1975): Observation of the Directional Spectrum of Ocean Waves Using a Clover-leaf Buoy, Jour. Physical Oceanogr., Vol.5, No.4, pp.750 - 760.
- 6) Tanimoto, K. and Y. Yoshimoto (1982): Factors of Wave Reflection from Vertical Slit Caisson Wall, Proc. 29th Japanese Conf. Coastal Eng., pp.389 - 393.